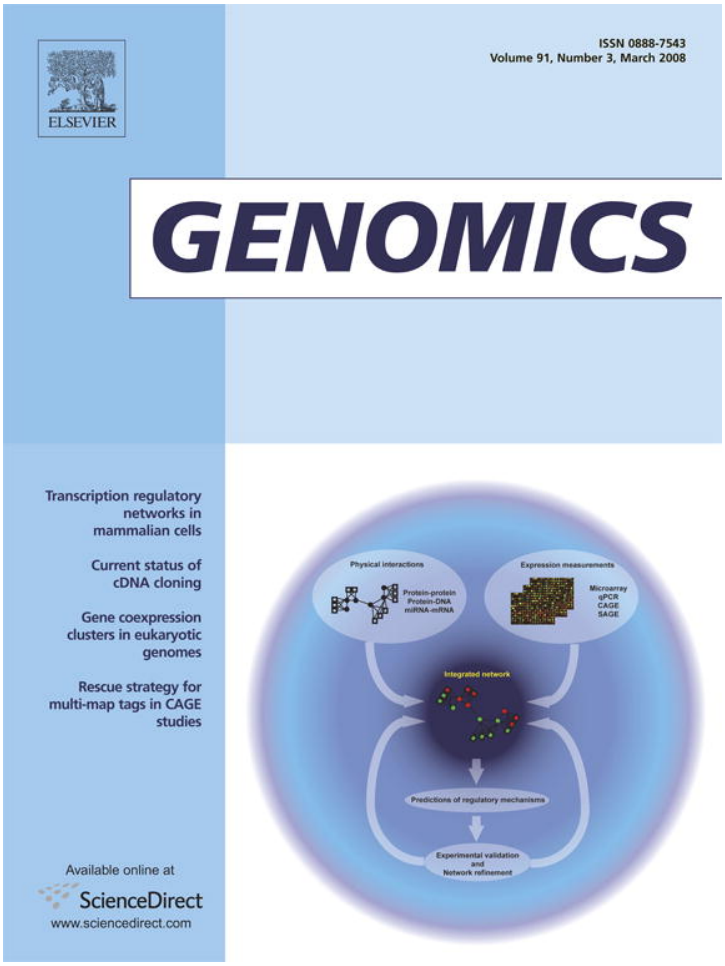

Available online at www.sciencedirect.com
ScienceDirect
Genomics 91 (2008) 289–300
GENOMICS
www.elsevier.com/locate/ygeno

Transcriptional profiling and inhibition of cholesterol biosynthesis in human T lymphocyte cells by the marine toxin azaspiracid

Michael J. Twiner [a,*], James C. Ryan [a], Jeanine S. Morey [a], Kent J. Smith [b], Samar M. Hammad [c], Frances M. Van Dolah [a], Philipp Hess [d], Terry McMahon [d], Masayuki Satake [e], Takeshi Yasumoto [f], Gregory J. Doucette [a]

[a] *Marine Biotoxins Program, Center for Coastal Environmental Health and Biomolecular Research, NOAA/National Ocean Service, 219 Fort Johnson Road, Charleston, SC 29412, USA*
[b] *Department of Biochemistry and Molecular Biology, Medical University of South Carolina, Charleston, SC 29401, USA*
[c] *Department of Cell Biology and Anatomy, Medical University of South Carolina, Charleston, SC 29401, USA*
[d] *Biotoxin Chemistry, Marine Institute, Rinville, Oranmore, Ireland*
[e] *Graduate School of Agricultural Science, Tohoku University, Sendai, Japan*
[f] *Japan Food Research Laboratory, Tama Laboratory, Nagayama, Tama, Tokyo, and Okinawa Health Biotechnology Research Development Center, Gushikawa, Okainawa, Japan*

Received 6 March 2007; accepted 20 October 2007
Available online 11 January 2008

Abstract

Azaspiracid-1 (AZA-1) is a marine biotoxin reported to accumulate in shellfish from several countries, including eastern Canada, Morocco, and much of western Europe, and is frequently associated with severe gastrointestinal human intoxication. As the mechanism of action of AZA-1 is currently unknown, human DNA microarrays and qPCR were used to profile gene expression patterns in human T lymphocyte cells following AZA-1 exposure. Some of the early (1 h) responding genes consisted of transcription factors, membrane proteins, receptors, and inflammatory genes. Four- and 24-h responding genes were dominated by genes involved in de novo lipid biosynthesis of which 17 of 18 involved in cholesterol biosynthesis were significantly up regulated. The up regulation of synthesis genes was likely in response to the ca. 50% reduction in cellular cholesterol, which correlated with up regulated protein expression levels of the low-density lipoprotein receptor. These data collectively detail the inhibition of de novo cholesterol synthesis, which is the likely cause of cytotoxicity and potentially a target pathway of the toxin.

Keywords: Azaspiracid-1; Cholesterol; Fatty acid; Gene expression; Harmful algal bloom; Immunoblot; Low-density lipoprotein receptor; T lymphocyte cells; Microarray; Shellfish toxin

Azaspiracids (AZA) are polyether marine toxins (Fig. 1) that were first detected in mussels (*Mytilus edulis*) from Ireland following a 1995 outbreak of gastrointestinal illness and have since been detected in other bivalve species, including oysters (*Crassostrea gigas, Ostrea edulis*), scallops (*Pecten maximus*), clams (*Tapes philippinarum*), cockles (*Cardium edule*), and razor clams (*Ensis siliqua*) [1–3]. Cases of AZA intoxication and/or contaminated shellfish have been documented in several other European countries, including the United Kingdom, Norway, The Netherlands, France, Spain, and Italy [4–7] and more recently in eastern Canada (M. Quilliam, personal communication) as well as Morocco [8]. In Europe, a regulatory limit of 160 μg AZA-1 equivalents/kg whole shellfish flesh has been set to protect human health (Regulation EC 853/2004). Recently, from July to December 2005, levels of AZA exceeding this regulatory limit were detected in mussels from production areas along the west coast of Ireland [9] and in some production areas AZA levels remained above the regulatory limit for more than 9 months.

Following human consumption of AZA-contaminated shellfish, there is a rapid onset of symptoms that include nausea, vomiting, severe diarrhea, and stomach cramps [10,11]. Although the human symptoms resemble those of diarrhetic

* Corresponding author. Fax: +1 843 762 8700.
E-mail address: Mike.Twiner@noaa.gov (M.J. Twiner).

0888-7543/$ - see front matter © 2007 Elsevier Inc. All rights reserved.
doi:10.1016/j.ygeno.2007.10.015

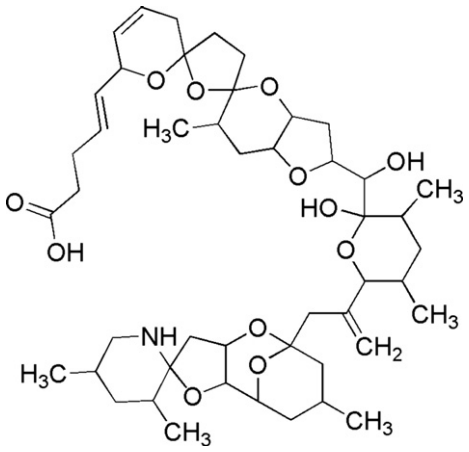

Fig. 1. Structure of azaspiracid-1 (AZA-1).

shellfish poisoning (DSP), the illness has subsequently been named azaspiracid poisoning (AZP) [12,13], reflecting the causative toxin family. Murine intraperitoneal injections induce symptoms such as fatigue, paralysis, labored breathing, and death as soon as 35 min postinjection [10,11]. Pathological effects include histological alterations in the liver, pancreas, spleen, and necrotic lymphocytes in the thymus. Experiments in which mice were chronically dosed with AZA-1 (oral administration of 5–50 μg/kg) demonstrated that AZA-1 exposure induces gastrointestinal inflammation, including accumulation of fluid, necrosis, and edema in the lamina propria of the midintestinal tract, as well as fusion and shortening of villi. Necrosis of T and B lymphocytes was also documented in the spleen and thymus, as well as fatty changes in the liver, hyperplasia of the epithelial lining in the stomach, and tumors in the lungs [5,13,14]. Due to the incidence of lung tumors, AZA-1 is currently being investigated as a potential carcinogen, particularly since it has been shown recently to act as a teratogen in fish embryos [15].

Studies to determine the mechanism of action of AZA have been conducted by several investigators using in vitro techniques. Although AZP symptoms in humans are similar to those of DSP, AZA-1 does not alter the activities of protein phosphatase-1 (PP1) or PP2A [16], both known targets for DSP toxins, indicating a different mechanism of action for AZA. Cytotoxicity testing of seven mammalian cell lines has shown that AZA-1 is cytotoxic to all tissue types examined (lymphoid, kidney, lung, neuronal, and pituitary cells), with EC_{50} values in the low nanomolar range (0.9–16.8 nM) [16]. Interestingly, immune-type cells appeared to be most sensitive to the cytotoxic effects of AZA-1, correlating with in vivo pathological observations [5,14,17]. In particular, the morphology and cytoskeleton of a human T lymphocyte cell line (Jurkat) were distinctly affected by AZA-1. Similar changes have also been documented by Roman et al. [18], in that AZA-1 reduced cellular F-actin content in a nonapoptotic manner following the elevation of cytosolic calcium and cAMP levels. Recent work by Vilarino et al. [19] has also revealed effects of AZA-1 toward cytoskeletal components, while Ronzitti et al. [20] reported that AZA-1 causes fragmentation of E-cadherin, a membrane protein involved in cell–cell adhesion. To investigate further the potential mechanism(s) of action of AZA-1, we employed a whole-genome expression microarray to assess the differential expression of >37,000 genes at three time points following the exposure of T lymphocyte cells to AZA-1 over 24 h. A pathway of interest was identified from the gene expression data and confirmed by qPCR, immunoblots, and substrate analysis.

Results

To assess the response of T lymphocyte cells to AZA-1, gene expression in Jurkat cells following exposure to AZA-1 (10 nM) was compared to basal gene expression in control cells exposed to equivalent amounts of the methanolic vehicle at 1, 4, and 24 h. As illustrated in Fig. 2, this concentration had significant effects on both cell morphology and cytotoxicity. After 24 h of AZA-1 exposure, the altered morphology of T lymphocyte cells, including cell rounding and retraction of pseudopodia, was characteristic of a cytotoxic response. This was confirmed by detecting the release of the cytosolic enzyme glucose-6-phosphate dehydrogenase, which is also corroborated by our previous study [16].

Signature genes and clusters

Features from the composite gene expression microarrays were classified as differentially expressed, or "signature," if they possessed a p value ≤ 0.01 using the Rosetta error model and weighted averaging. An overview of the signature feature gene data can be found in Supplementary Table 1. Signature features with an absolute differential expression of >1.5 (=0.58 $\log_2$ ratio value) and p value $\leq 10^{-4}$ were analyzed further and resulted in three distinct clusters containing a total of 437 differentially expressed genes (Fig. 3). Cluster 1 (highly up regulated features) contained 92 genes, cluster 2 (moderately up regulated) contained 202 genes, and cluster 3 (moderately down regulated) contained 143 genes. Details of these features are shown in Supplementary Tables 2, 3, and 4, respectively. At least 38 genes within these clusters are involved directly in lipid regulation (i.e., transcription factors, enzymes for cholesterol or fatty acid synthesis, elongation, modification, etc.). The majority of these genes were from cluster 1 (33 of 38), and 5 genes were from cluster 2. Table 1 illustrates the details of these lipid-related genes in which it is clear that most were significantly up regulated at the 4- and 24-h time points, but were not differentially expressed at 1 h. In some instances, multiple yet different probes on the array query the same gene; as a result, some genes appear more than once in Table 1. These data are only a subset of the gene expression array data; however, all raw gene expression data are available at Gene Expression Omnibus (GEO; http://www.ncbi.nlm.nih.gov/geo/; GEO Accession No. GSE5346).

Although clusters 1 and 2 were dominated by up regulated lipid-related genes, cluster 1 also included genes related to glucose metabolism (i.e., insulin-induced gene 1), cell signaling (i.e., C/EBP-induced protein), and cell growth (i.e., cyclin G2)

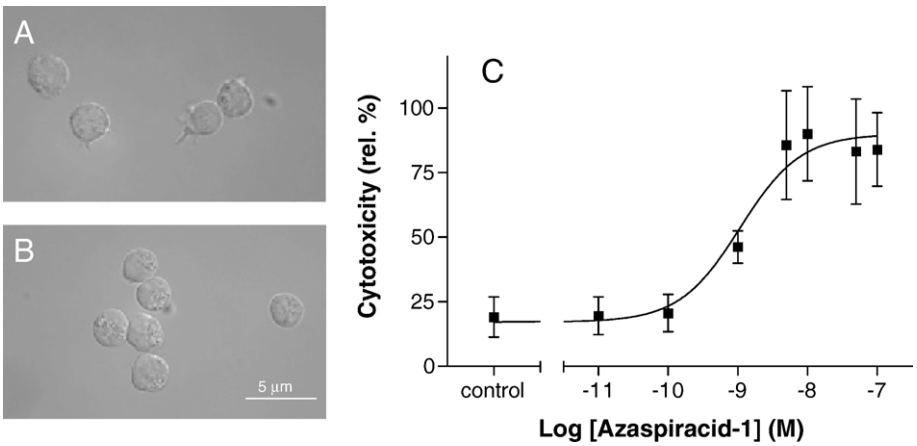

Fig. 2. Effects of azaspiracid-1 on cell morphology and cytotoxicity of human T lymphocyte cells. Cells were continuously exposed to either (A) methanol (0.1% final) or (B) AZA-1 (10 nM) before the photomicrographs were taken. (C) Cytotoxicity was determined with increasing concentrations of AZA-1 (10^{-11} to 10^{-7} M) for 24 h before cellular lysis was assessed via release of glucose-6-phosphate dehydrogenase (G6PD). G6PD release was quantified and normalized as a function of total G6PD (100% cytotoxicity). Cytotoxicity data are means ± SE in triplicate wells for three independent experiments. Controls were treated with equivalent amounts of the methanol vehicle. An EC_{50} value of 1.1 nM was determined by a variable slope sigmoidal regression analysis using GraphPad Prism software (version 4.00).

(Supplementary Table 2). Cluster 2 contained many genes related to glucose metabolism (i.e., pyruvate dehydrogenase kinase), cell signaling (i.e., interferon-stimulated gene, intercellular adhesion molecule 2, G-protein-coupled receptors, transcription factors), ion transport (i.e., ATPases, potassium channel), and cell death/apoptosis (i.e., BCL2-interacting protein 3, p53-inducible nuclear protein 1) (Supplementary Table 3). The typically down regulated genes within cluster 3 were represented by genes involved in cell signaling (i.e., glucagon receptor, WNT frizzled homolog 9, neuronatin), cell growth (i.e., cyclin B2, cyclin-dependent kinase inhibitor 3), stress response (i.e., heat shock proteins), and translation (i.e., mitochondrial ribosomal proteins) (Supplementary Table 4). It should also be noted that preliminary gene expression analysis of cells exposed to 1 nM AZA-1 also elicited similar transcriptional patterns (data not shown).

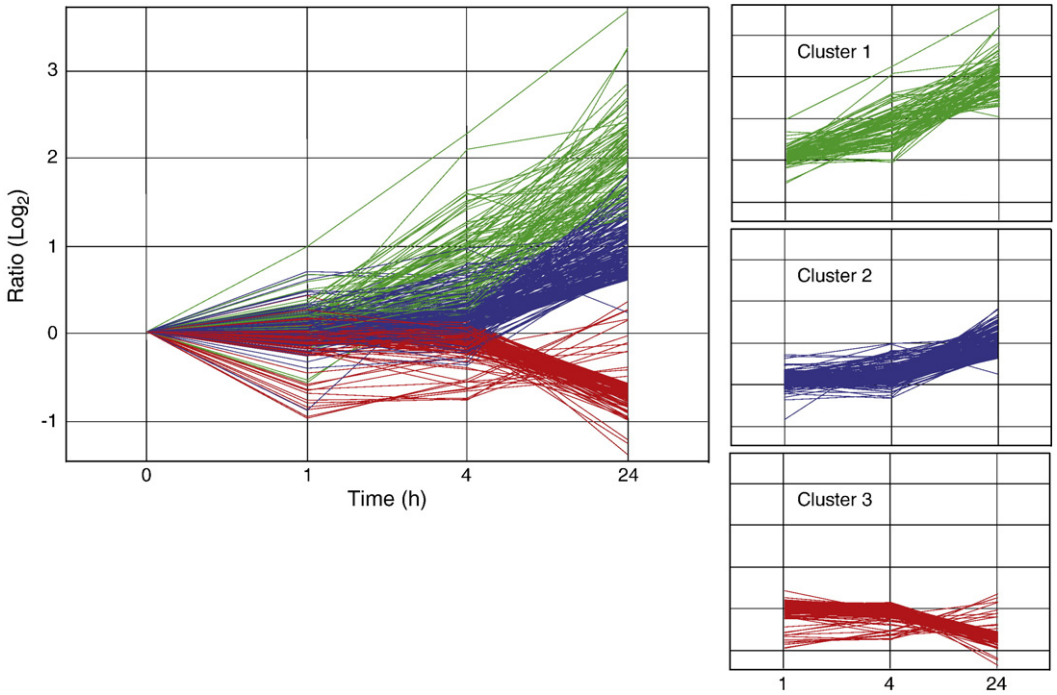

Fig. 3. Clustered trend set. T lymphocytes were exposed to AZA-1 (10 nM) for 1, 4, and 24 h and differentially expressed genes identified. Genes were clustered using a *K*-means algorithm with Euclidean distance measurements (fold change ≥ 1.5 or ≤ −1.5; $p \leq 10^{-4}$) and resulted in 437 differentially expressed genes. Three clusters were identified: cluster 1 (green) contained 92 genes, cluster 2 (blue) contained 202 genes, and cluster 3 (red) contained 143 genes. Thirty-eight genes (33 from cluster 1; 5 from cluster 2) were involved in lipid regulation (see Table 1). Data are plotted as ratio $\log_2$ values.

Table 1
Differentially expressed genes involved in lipid regulation

Accession or Agilent probe No.	Sequence description	1 h		4 h		24 h		Cluster
		Ratio	*p* value	Ratio	*p* value	Ratio	*p* value	
NM_014762	24–Dehydrocholesterol reductase (DHCR24)	1.02	0.83	1.81	2.90×10^{-6}	4.13	7.69×10^{-23}	1
NM_000859	HMG–coenzyme A reductase (HMGCR)	1.06	0.40	2.74	3.43×10^{-21}	5.66	$<1.0\times10^{-45}$	1
BC000297	HMG–coenzyme A synthase 1 (HMGCS1)	1.03	0.76	2.78	2.75×10^{-40}	5.04	2.14×10^{-34}	1
AK095492	HMGCS1	1.02	0.83	4.22	$<1.0\times10^{-45}$	5.21	8.46×10^{-9}	1
NM_001360	7–Dehydrocholesterol reductase (DHCR7)	1.00	0.98	2.26	2.21×10^{-19}	5.42	6.41×10^{-25}	1
NM_005891	Acetyl–coenzyme A acetyltransferase 2 (ACAT2)	1.08	0.41	2.03	$<1.0\times10^{-45}$	4.83	$<1.0\times10^{-45}$	1
AF356877	ACAT2	0.98	0.67	1.79	1.47×10^{-6}	5.48	$<1.0\times10^{-45}$	1
NM_024090	ELOVL family, fatty acid elongation (ELOVL6)	1.20	0.50	1.08	0.84	3.02	1.00×10^{-4}	1
NM_006579	Emopamil–binding protein (sterol isomerase) (EBP)	1.03	0.70	1.49	2.59×10^{-15}	3.63	$<1.0\times10^{-45}$	1
NM_002004	Farnesyl diphosphate synthase (FDPS)	0.98	0.70	1.46	4.00×10^{-5}	4.57	$<1.0\times10^{-45}$	1
A_32_P95223	FDPS	1.03	0.79	1.22	0.14	4.33	$<1.0\times10^{-45}$	1
XM_291508	FDPS	0.99	0.94	1.27	0.03	3.96	$<1.0\times10^{-45}$	1
NM_004462	Farnesyl diphosphate farnesyltransferase 1 (FDFT1)	1.00	0.95	1.61	1.87×10^{-12}	2.45	8.62×10^{-12}	1
NM_013402	Fatty acid desaturase 1 (FADS1)	0.88	0.22	1.48	7.71×10^{-12}	3.16	$<1.0\times10^{-45}$	1
NM_013402	FADS1	1.08	0.48	1.74	5.57×10^{-28}	4.02	2.77×10^{-41}	1
NM_004265	Fatty acid desaturase 2 (FADS2)	1.02	0.81	1.37	5.19×10^{-8}	3.24	$<1.0\times10^{-45}$	1
NM_016371	Hydroxysteroid (17–β) dehydrogenase 7 (HSD17B7)	1.02	0.92	1.75	1.50×10^{-4}	2.47	2.10×10^{-32}	1
NM_016371	HSD17B7	1.16	0.31	2.03	1.54×10^{-7}	2.52	2.48×10^{-8}	2
NM_004508	Isopentenyl–diphosphate ä isomerase (IDI1)	1.01	0.94	2.24	3.00×10^{-24}	4.25	3.07×10^{-12}	1
AK096769	Lanosterol synthase (LSS)	0.94	0.89	1.61	0.38	4.85	4.45×10^{-9}	1
NM_002340	LSS	0.95	0.53	2.19	3.00×10^{-5}	4.90	9.21×10^{-12}	1
AK096769	LSS	1.01	0.98	1.86	0.03	4.33	5.02×10^{-17}	1
NM_002340	LSS	1.10	0.34	2.22	2.00×10^{-5}	7.08	1.29×10^{-16}	1
NM_000527	Low–density lipoprotein receptor (LDLR)	1.10	0.07	2.22	2.24×10^{-10}	3.47	$<1.0\times10^{-45}$	1
NM_181726	LDLR–related–binding protein (LRP2BP)	0.99	0.96	1.15	0.14	1.87	5.02×10^{-10}	2
NM_002461	Mevalonate (diphospho) decarboxylase (MVD)	0.83	0.16	1.14	0.55	3.02	4.42×10^{-9}	1
X75311	Mevalonate kinase (MVK)	0.96	0.59	1.92	2.62×10^{-42}	3.61	1.01×10^{-43}	1
NM_022776	Oxysterol–binding protein–like 11 (OSBPL11)	0.99	0.90	1.18	0.09	1.75	9.00×10^{-5}	2
NM_003129	Squalene epoxidase (SQLE)	1.18	0.01	2.37	4.26×10^{-27}	2.92	1.21×10^{-6}	1
NM_139164	START domain–containing 4 (STARD4)	1.13	0.33	1.99	8.30×10^{-19}	5.15	$<1.0\times10^{-45}$	1
NM_005063	Stearoyl–CoA desaturase (SCD)	0.97	0.76	1.95	4.24×10^{-31}	2.99	2.43×10^{-9}	1
NM_005063	SCD	1.04	0.80	1.47	0.07	9.26	2.64×10^{-27}	1
AF132203	SCD	1.11	0.29	1.75	2.30×10^{-4}	3.93	$<1.0\times10^{-45}$	1
NM_004176	Sterol reg. element–binding transcription factor 1 (SREBF1)	1.01	0.93	1.23	0.02	1.88	6.06×10^{-15}	2
NM_004599	Sterol reg. element–binding transcription factor 2 (SREBF2)	0.92	0.49	0.99	0.90	1.70	1.32×10^{-6}	2
NM_006745	Sterol–C4–methyl oxidase–like (SC4MOL)	1.23	0.10	2.95	6.71×10^{-14}	3.00	2.70×10^{-6}	1
NM_006918	Sterol–C5–desaturase (SC5DL)	1.07	0.60	2.14	1.12×10^{-12}	2.80	2.00×10^{-5}	1
BC012333	SC5DL	0.96	0.68	1.99	1.80×10^{-7}	2.88	2.58×10^{-38}	1

T lymphocyte cells were exposed to AZA–1 (10 nM) for 1, 4, and 24 h and differentially expressed genes from Fig. 3 that are involved with lipid regulation are shown here. Multiple differentially expressed values for the same gene may be given due to multiple probes made against different locations on a single sequence for a given transcript.

qPCR

Eleven genes involved with cholesterol biosynthesis were selected for verification by qPCR, and an α-tubulin-like gene (GenBank Accession No. NM_145042) was chosen for normalization purposes. The α-tubulin-like gene exhibited no significant changes in expression in either the microarray or the qPCR analysis (data not shown). The changes (i.e., magnitude and direction) in many of the cholesterol biosynthesis genes detected by microarrays were confirmed by qPCR (Fig. 4). Pearson's correlation coefficient between the microarray and the qPCR gene expression ratios were for all data 0.9173, $n=24$, $p\leq0.0001$; for 4 h data 0.7538, $n=12$, $p=0.0046$; and for 24 h data 0.9436, $n=12$, $p\leq0.0001$. In addition, the direction of regulation was conserved for 23 of 24 (96%) genes. In the one instance in which the direction was not conserved (i.e., PMVK), the fold change was less than 1.2 by both methods. For additional qPCR and microarray comparisons from this study, refer to Morey et al. [21].

Mapping gene expression patterns for the cholesterol biosynthesis pathway using GenMapp

Analysis of the gene expression data by MappFinder yielded a list of pathways and/or cellular processes sorted by *Z* score that were identified as having a higher proportion of differentially expressed genes than expected. Fatty acid, lipoprotein, and cholesterol pathways were calculated to have some of the highest *Z* scores (≥4.0) for the 4- and 24-h time points (data not shown). Gene expression values at 4 and 24 h have been plotted onto the cholesterol biosynthesis pathways for visualization (Fig. 5). At 4 h following the addition of AZA-1, 14 of

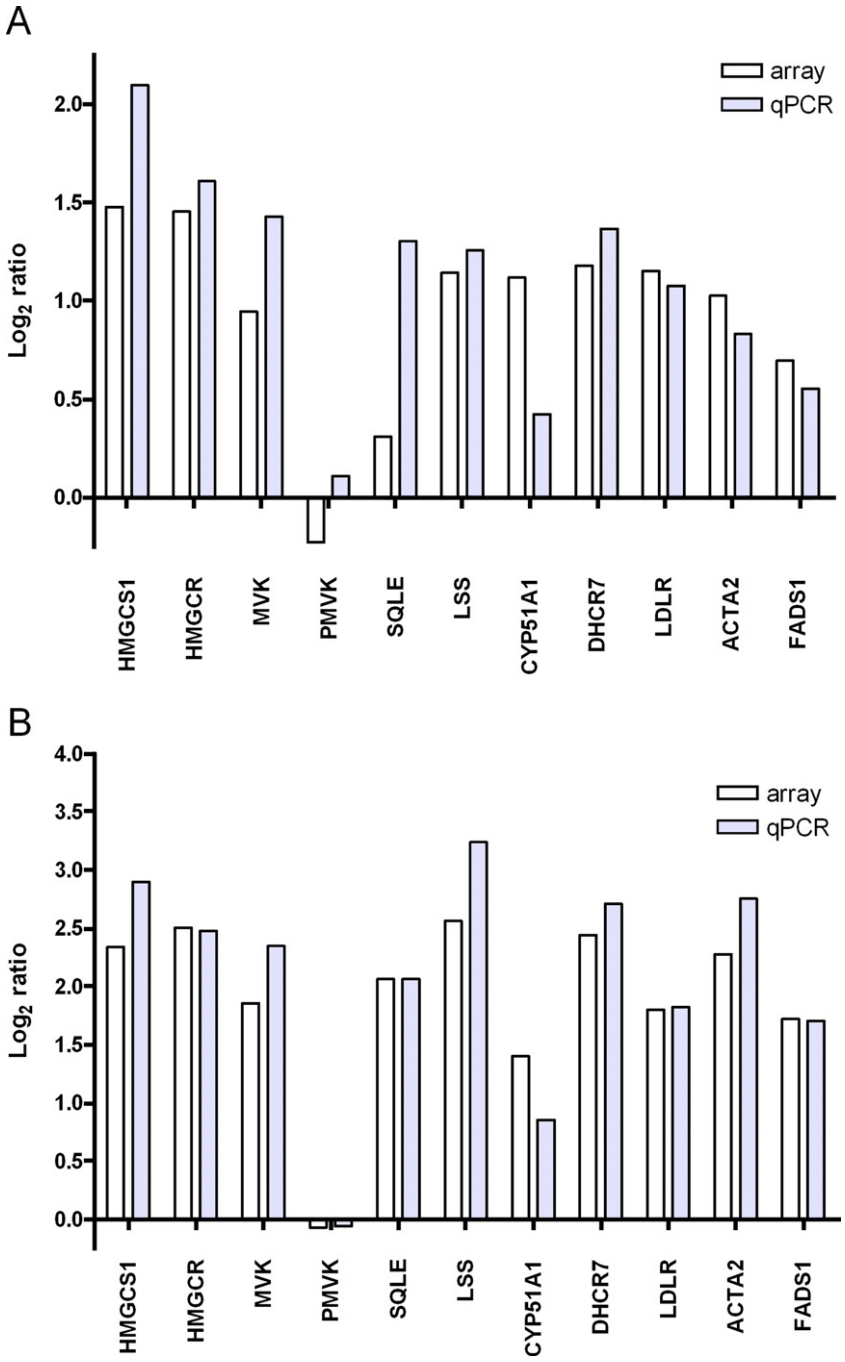

Fig. 4. Quantitative PCR validation of arrays. Eleven selected genes from the lipid biosynthesis pathways were validated by qPCR at (A) 4 and (B) 24 h. Array and PCR expression data are expressed as $\log_2$ ratio. The Pearson's correlation coefficient between the microarray and the qPCR gene expression ratios were for all data 0.9173, $n=24$, $p \leq 0.0001$; for 4 h data 0.7538, $n=12$, $p=0.0046$; and for 24 h data 0.9436, $n=12$, $p \leq 0.0001$. Full gene names and accession numbers are shown in Fig. 5.

the 16 genes illustrated in the cholesterol biosynthesis pathway were significantly up regulated (between 1.5- and 4.2-fold) for at least one of the gene isoforms (Fig. 5). At 24 h, 15 of the 16 genes (ranging between 2.3- and 7.1-fold) were significantly up regulated. Genes that encode ACAT2 and LDLR were also significantly up regulated at both time points. Although not illustrated, many of the genes involved in fatty acid synthesis were also significantly up regulated at 4 and 24 h, in addition to INSIG1, INSIG2, SREBP1, and SREBP2 (see Supplementary Tables 2 and 3).

Immunoblot analysis of LDLR

T lymphocyte cells exposed to AZA-1 were assessed for differential expression of the low-density lipoprotein receptor (LDLR) by immunoblot analysis. Although control cells displayed little change in the expression of LDLR over the 24-h time course, cells exposed to AZA-1 (1 or 10 nM) had significantly higher levels of LDLR in a time- and concentration-dependent manner (Fig. 6). LDLR in the 1 nM AZA-1 treatments was significantly up regulated at 12 h (~2.5-fold), whereas in the

10 nM treatments it was up regulated at 4 h (~1.5-fold). Data for the 10 nM treatments at 24 h were not available because of cytotoxicity and an insufficient amount of protein available for loading onto the gel. Serum-starved cells (−FBS) were used as positive controls for up regulated LDLR (data not shown).

Quantitative analysis of cellular cholesterol

T lymphocyte cells were exposed to AZA-1 (1 or 10 nM) for 4, 12, or 24 h for quantification of free and esterified cellular cholesterol. Control cells normalized to ng/μg protein displayed some reductions in total cellular cholesterol levels over the period of the experiment, likely due to limiting extracellular serum as cell numbers increased (Fig. 7). Total cholesterol levels (mean ± SE, $n = 3$) in the controls were 9.1 ± 0.4 ng cholesterol/μg protein or 891 ± 16 fg/cell. Treatments with AZA-1 caused significant ($p < 0.001$) reductions in cellular cholesterol levels to 4.8 ± 0.2 ng cholesterol/μg protein (or 737 ± 85 fg/cell), for the 1 nM treatment, and 4.8 ± 0.4 ng cholesterol/μg protein (or 711 ± 16 fg/cell) for the 10 nM treatment. Differences in free or esterified cholesterol were not detected between controls and treatments, in which esterified cholesterol consistently accounted for 10 to 15% of the total cholesterol content (data not shown).

Discussion

Azaspiracid accumulation in shellfish and its potential human health risk to seafood consumers is an ongoing issue in Europe and appears to be an emerging problem in African and North American waters. However, our lack of understanding of the AZA-1 mechanism of action has hindered our ability to assess both its acute and its chronic health effects. This study is the first to assess the in vitro effects of AZA-1 on gene expression, which in turn, has demonstrated conclusively the inhibitory effects of AZA-1 on de novo cholesterol biosynthesis.

Biological pathway analysis following T lymphocyte cell exposure to AZA-1

Analysis of gene expression patterns using whole human genome microarrays revealed several biological pathways that appear to be targeted when T lymphocyte cells are exposed to AZA-1. These pathways include, but are likely not limited to, cholesterol and fatty acid synthesis, the insulin/glucagon pathway, the WNT signaling pathway, and other pathways that are involved in inflammation, ion channel activities, the cytoskeleton, and cell growth/division.

Cholesterol and fatty acid synthesis pathway

Many of the genes identified in clusters 1 and 2 are necessary for cholesterol biosynthesis and were up regulated at the 4- and 24-h time points. AZA-1 elevated transcriptional levels of 15 of 16 genes involved in the synthesis of cholesterol from acetyl-CoA, which is similar to inhibition of the cholesterol biosynthesis pathway caused by statins. Skeletal muscle cells exposed to various statins over 24 h were shown to up regulate many cholesterol synthesis genes (i.e., LSS, HMGCR, SQLE, HMGCS1) [22]. The remarkable clustering of up regulated genes of similar function and regulation by AZA-1 prompted further experimental examination of LDLR.

Found within the membrane of many cell types, LDLR is typically involved in regulating the level of cholesterol in the blood. This receptor binds with and internalizes low-density lipoproteins delivering cholesterol for cellular use and storage. Following internalization, LDLRs are recycled back to the outer membrane. LDLRs play a critical role in regulating cholesterol in which their translocation and transcriptional expression are inversely proportional to intracellular cholesterol levels. HMGCR inhibitors such as statins [23,24] are well known to lower cellular cholesterol levels with a concomitant elevation in LDLR activity [25]. LDLR protein expression is clearly shown to be up regulated in a time- and concentration-dependent fashion by AZA-1 relative to the control cells.

Protein LDLR up regulation is consistent with both the LDLR transcriptional response and the decreased levels of cellular cholesterol induced by AZA-1. Inhibition of total cellular cholesterol synthesis was clearly illustrated by an almost 50% decrease from time-matched control cells for each AZA-1 concentration. The total cholesterol level in controls cells was ~8.5 ng cholesterol/μg protein, whereas in both 24-h treatments levels had dropped to ~4.6 ng cholesterol/μg protein. Although future experimentation will be needed to assess further the effects of additional AZA-1 concentrations on cholesterol levels in Jurkat cells, the effects of AZA-1 on the cholesterol biosynthetic pathway appear to be consistent with those of statins and inhibition of de novo cholesterol synthesis. Although speculative, a possible site of inhibition may involve phosphomevalonate kinase (PMVK; GenBank Accession No. NM_006556), the lone gene in this pathway that was not up regulated by AZA-1. PMVK catalyzes the phosphorylation of mevelonate-5-P into mevalonate-5-PP and has been shown to be transcriptionally controlled in response to cellular sterol levels [26]; however, there may be a posttranscriptional control not detectable by the current gene expression study.

Genes required for enzymatic synthesis of fatty acids were also up regulated in a time-dependent manner at 4 and 24 h. In addition to the fatty acid synthesis genes, a variety of other sterol regulatory genes such as SREBP and INSIG1 (insulin-induced gene 1) were up regulated, potentially eliciting control of the fatty acid and/or cholesterol synthesis pathways [27–31]. INSIG1 is essential for feedback regulation of cholesterol synthesis [27]. Similarly, sucrose-induced vacuolation of human fibroblast cell lines has been shown to up regulate many of the same genes relating to fatty acid and cholesterol synthesis [32] that were observed in the present study. These authors suggested that cholesterol, fatty acid, and vesicle-trafficking genes are up regulated as a function of cellular swelling and increased cellular demand for sterol and lipid membrane components. Although this mechanism of up regulated lipid gene expression cannot be excluded, cell swelling does not appear to be a common characteristic of AZA-1-induced cytotoxicity (see Fig. 2 and Twiner et al. [16]). Mutated fibroblasts lacking a functional NADPH steroid dehydrogenase-like (NSDHL) gene, which is necessary

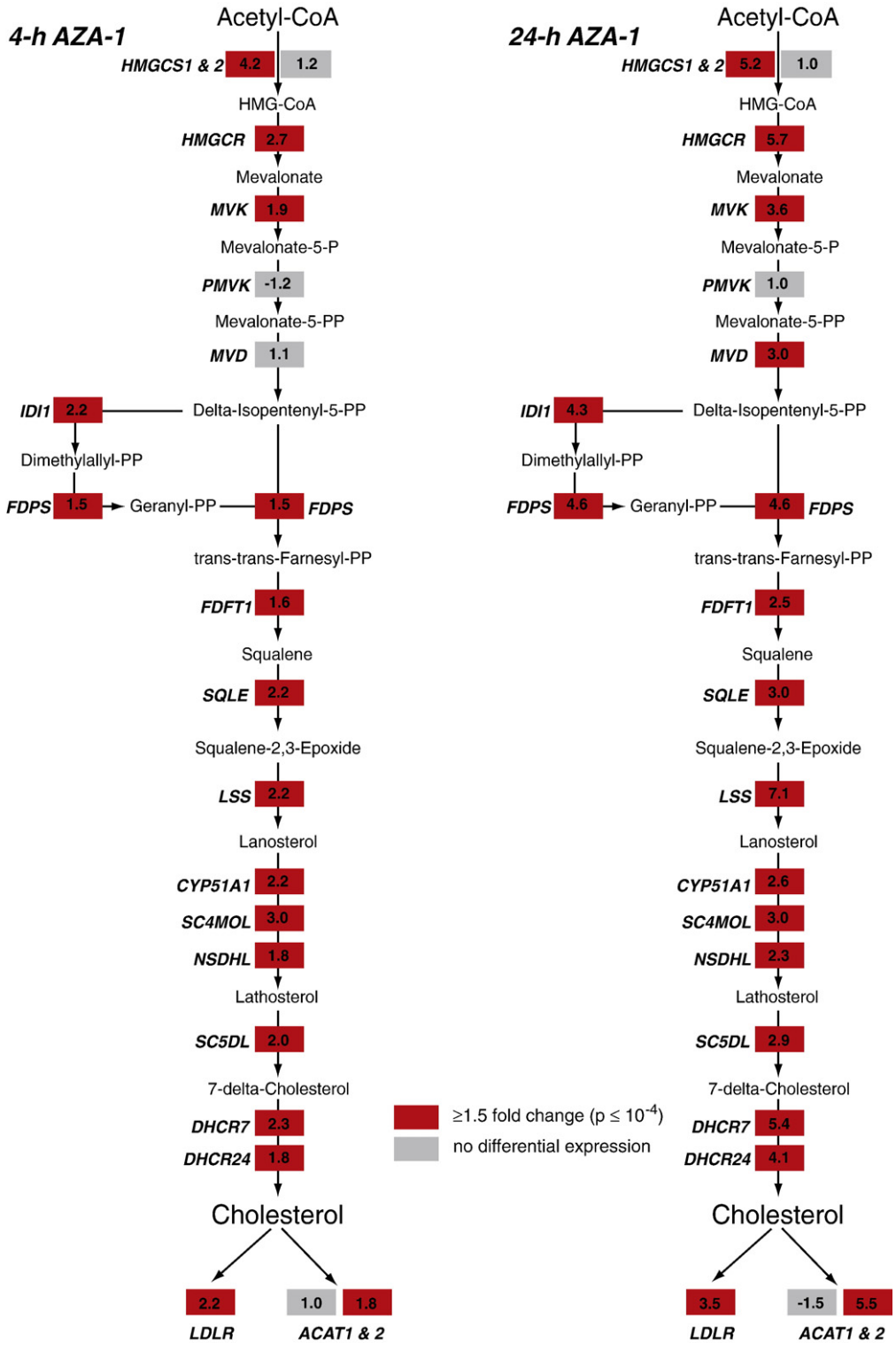

Fig. 5. Effects of azaspiracid-1 on cholesterol biosynthesis gene expression. T lymphocyte cells were exposed to AZA-1 (10 nM) for 4 and 24 h. Each box represents a gene isoform capable of expressing a protein involved in the biosynthesis of cholesterol from acetyl-CoA. Each box is labeled with an abbreviated gene name in bold italic and the number represents the fold change relative to the time-matched control expression (fold change = 1). Normal font represents the substrates. Gene expression levels are categorized as significant (red) or not significant (gray) according to fold change (≥ 1.5-fold) and p value ($\leq 10^4$). Biochemical pathway maps were generated using Gene Map Annotator and Pathway Profiler 2.0 (GenMapp). Gene names are HMGCS1, 3-hydroxy-3-methylglutaryl–coenzyme A synthase 1; HMGCR, 3-hydroxy-3-methylglutaryl-coenzyme A reductase; MVK, mevalonate kinase; PMVK, phosphomevalonate kinase; MVD, mevalonate (diphospho) decarboxylase; IDI1, isopentenyl-diphosphate δ-isomerase 1; FDPS, farnesyl diphosphate synthetase; SQLE, squalene epoxidase; LSS, lanosterol synthase; CYP51A1, cytochrome P450, family 51, subfamily A, polypeptide 1 (lanosterol 14 α-demethylase); SC4MOL, sterol-C4-methyl oxidase-like; NSDHL, NAD(P)-dependent steroid dehydrogenase; SC5DL, sterol-C5-desaturase-like; DHCR7, 7-dehydrocholesterol reductase; DHCR24, 24-dehydrocholesterol reductase; LDLR, low-density lipoprotein receptor; ACAT, acetyl-coenzyme A acetyltransferase 2.

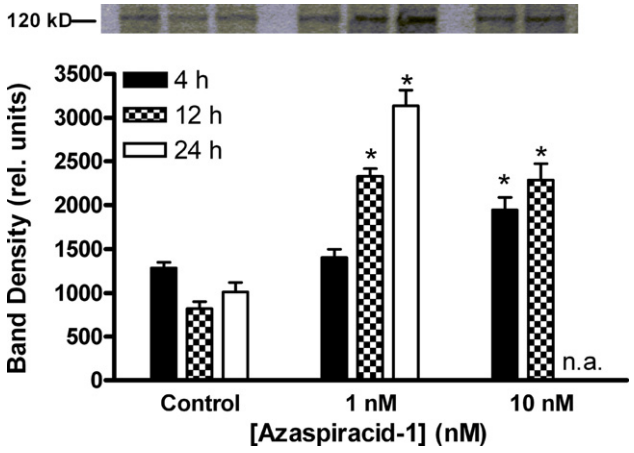

Fig. 6. Effect of azaspiracid-1 on levels of LDLR. Immunoblot analysis was used to evaluate the expression of LDLR in detergent extracts of azaspiracid-treated T lymphocyte cells. Equal amounts of protein (40 μg) were separated by SDS–PAGE under reducing conditions. A representative immunoblot scan at 120 kDa is illustrated. Scanning densitometry was performed using NIH ImageJ and graphical data (means ± SE) are representative of three independent experiments. Data from the 10 nM treatment at 24 h were not available (n.a.) because of cytotoxicity and insufficient amount of protein to be loaded. *Significant difference at $p < 0.001$ relative to corresponding time-matched controls.

for cholesterol synthesis, revealed a high degree of up regulated cholesterol and fatty acid synthesis gene expression [31], not unlike the data presented herein. Similarly, cytochrome P450 knockout mice were shown to have elevated expression levels of multiple lipid synthesis genes [33], for which cytochrome enzyme oxidation is one of the final steps in cholesterol synthesis.

The transcription factor family of CCAAT/enhancer binding proteins (C/EBP) are key regulators of adipogenesis (i.e., fatty acid and cholesterol synthesis) and contain a highly conserved DNA-binding region that is very similar to that of SREBPs [34]. C/EBPs are known to bind to a promoter region of the LDLR gene, inducing enhanced expression of this cholesterol receptor [35,36]. The induced expression of C/EBP by AZA-1 may therefore have enhanced the up regulation of fatty acid and cholesterol synthesis pathways observed in this study.

Alteration of the lipid biosynthesis pathway is consistent with reports of altered secondary messenger signaling [18], cytotoxicity [16], and developmental retardation [15] following AZA-1 exposure. Considering the dependence of membrane function on cholesterol levels [37], the effects of AZA-1 on particular membrane proteins such as claudins [9] and cadherins [20] reported by others are not unexpected. In the current study, the tight-junction protein claudin 5 was found to be down regulated at the 1-h time point (see supplementary data on the GEO database).

Insulin and glucagon signaling pathway

Many of the early responding (i.e., 1 h) genes tended to involve insulin and/or glucagon signaling pathways. Cellular energy stores, such as glucose, are well described modulators of these pathways [38], in which glucagon receptor expression is positively regulated by glucose and negatively regulated by glucagon, as well as agents that increase intracellular cAMP [39]. In human lymphocytes similar to the cells used in this study, AZA-1 was shown to increase intracellular Ca^{2+} and cAMP levels [18], potentially stimulating glucagon and/or cAMP-dependent pathways. The glucagon receptor gene (GCGR), in addition to neuronatin (NNAT), 6-phosphofructo-2-kinase/fructose-2,6-bisphosphatase (PFKFB3), and α-1,4-galactosyltransferase (A4GALT), are each involved with the glucagon/insulin pathways and were all down regulated at 1 h following exposure to AZA-1. The down regulation of neuronatin, a proteolipid membrane protein that responds positively to glucose-mediated insulin secretion [40], suggests stimulation of an insulin-opposing pathway. Similarly, PFKFB3, whose expression is also stimulated by insulin [41], was down regulated. The observed down regulation of CBP/MORF (cAMP-responsive element binding protein/monocytic leukemia zinc-finger protein-related factor), which is under partial cAMP control, can result in stimulated expression of lipogenic genes such as fatty acid synthase (FAS) and ATP-citrate lyase (ATP-CL) [42].

WNT signaling pathway

The WNT cell signaling pathway is a receptor-mediated pathway that tightly controls cell-to-cell communication and is known to be expressed in T lymphocyte cells [43]. As a regulator of cell proliferation and differentiation, the primary component of the WNT pathway is often, but not exclusively, β-catenin, a transcriptional cofactor with T cell factor (TCF)/lymphoid enhancer factor [44]. The T cell factor TCF7L2-HMG box and CBP, which were both down regulated by AZA-1, interact with β-catenin and have been implicated in transcriptional activation of the WNT pathway [45]. Interestingly, the Ras-related GTPase ARL7 and a receptor for the WNT pathway, Frizzled-9 (FZD9), were concurrently down regulated at 1 h and may represent gene expression feedback control following initial activation by AZA-1. LDLR has been shown to play an essential role in ligand-mediated WNT receptor signaling [46]. These findings may be intricately associated with the observations of Ronzitti et al. [20], revealing effects of AZA-1 on E-cadherins, which are known to affect the WNT pathway [44].

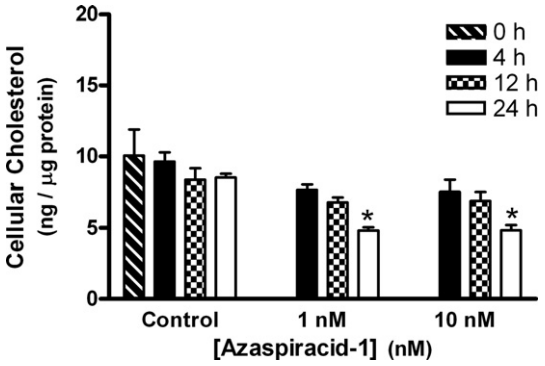

Fig. 7. Effect of azaspiracid-1 on cellular cholesterol levels. T lymphocyte cells were exposed to AZA-1 (1 or 10 nM) for 0, 4, 12, and 24 h. Control cells were exposed to equivalent amount of methanol (0.1% v/v). Data (means ± SE, $n = 3$) are expressed as total cellular cholesterol (free + ester) per unit of cellular protein. *Significant difference at $p < 0.001$ relative to time-matched controls.

Inflammatory, ion channel, cytoskeletal, and cell growth and division pathways

Exposure of cells and organisms to toxic agents often elicits an initial inflammatory response. Inflammatory genes such as the calcium-binding protein S100A4, tissue plasminogen activator, and cytochrome *c* oxidase (COX) IV were each down regulated at the 1-h time point after treatment with AZA-1. However, the calcium-binding protein S100A4 not only is involved in inflammation [47], but also enhances metastasis via effects on the cytoskeleton, apoptotic pathways, and plasminogens [48]. Although it does not appear that AZA-1 causes cytotoxicity via an apoptotic mechanism in lymphocyte cells (unpublished observation), it is clear that AZA-1 does induce dramatic effects on cytoskeletal elements [16,18].

Cytoskeletal changes induced by AZA-1 may also affect ion transport in cells as evidenced by up regulation of the chloride channel 6 (CLCN6) gene. CLCN expression was shown to be elevated during stress-induced periods of cellular swelling [32,49] and inflammation [50]. These voltage-gated chloride channels are known to aid in cholesterol trafficking [32] and ion balance. Chloride channels are co-localized with sarco/endoplasmic-reticulum Ca^{2+}pumps [51], which may account for the various effects of several AZA congeners on cytosolic calcium ion levels [18,52,53]. The effects of AZA-1 on CLCN6 gene expression might also be manifested as alterations in bioelectrical activity of spinal cord neurons that appears to involve the GABA neurotransmitter system [54] and may be linked directly to GABA receptor gating of chloride flux [55].

Cyclin G2 (CCNG2), an important gene for cell cycle mitotic control [56] known to be a target for the tumor suppressor protein p53, a regulator of cell growth and apoptosis [57], was significantly up regulated at 4 and 24 h. While p53 gene expression was not affected significantly by AZA-1, 5- to 14-fold up regulation of CCNG2 gene expression was observed in lymphocytes during periods of growth inhibition induced by dexamethasone, a known inducer of apoptosis [58]. Jurkat lymphocyte T cell growth inhibition induced by AZA-1, independent of cyclin G2 up regulation, has been clearly demonstrated, in which cytotoxicity and membrane disruption are protracted responses, typically after ≥ 18 h of continuous exposure [16].

Gene expression summary and conclusions

The majority of differentially expressed genes identified in this study tend to encode proteins with similar and/or related pathway functionality. T lymphocyte cells exposed to AZA-1 initially decreased the expression of transcription factor genes, genes related to membrane function and ion homeostasis, and key receptors and membrane proteins of the glucagon and WNT pathway. With continued AZA-1 treatment, dramatic and coordinated up regulation of nearly all cholesterol and fatty acid synthesis genes as well as the LDLR protein was observed, likely in response to reduced levels of cellular cholesterol. Interestingly, the glucagon/insulin, WNT, and cholesterol/fatty acid synthesis pathways are highly integrated based on their overlapping functionality, thereby suggesting that the effects elicited by AZA-1 may be via the toxin binding to a single, common target.

The T lymphocyte cells employed herein, a sensitive cell type identified previously from in vivo studies [5,14,17], clearly exhibited differential expression of the cholesterol biosynthesis pathway in concert with reduced intracellular levels of cholesterol and up regulated expression of the LDLR protein. While the mechanism of action for AZA-1 remains uncertain, other investigators have proposed the interaction of AZA-1 with membrane proteins such as claudins [9] and cadherins [20]. Our data are consistent with this argument, as many of these same genes showed differential expression. Altered levels of such membrane proteins could, in turn, be expected to affect both lipid biosynthesis gene expression and cytoskeletal rearrangement as observed in our current and past studies [16]. The data presented herein not only will serve to guide future hypothesis-driven investigations aimed at identifying the molecular target of AZA-1, but also can be used to develop exposure biomarkers and/or to assess the therapeutic potential of AZA-1.

Materials and methods

Azaspiracid purification

Azaspiracid was extracted from 2 kg of mussels (*M. edulis*) that were collected in 1996 from Killary Harbour, on the west coast of Ireland, and in 1999 from Bantry Bay, on the southwest coast of Ireland. Toxins were extracted and purified in 2001 (>93% pure by NMR and showed <1% impurity of other AZA subtypes/congeners), as previously described [16].

Cell lines and cytotoxicity

Human Jurkat E6-1 T lymphocyte cells (American Type Culture Collection TIB-152; Manassas, VA, USA) were grown as described in Twiner et al. [16]. Cytotoxicity was determined using the Vybrant cytotoxicity assay kit (Cat. No. V-23111; Invitrogen, Carlsbad, CA, USA) as per the manufacturer's instructions. Photomicrographs of unfixed cells were taken using an Axiovert S100 epifluorescence microscope (Carl Zeiss, Inc., Thornwood, NY, USA). For each experiment ($n=3$ biological replicates), between 1.2 and 10.6×10^6 cells were resuspended in fresh RPMI medium supplemented with FBS (10%) and allowed to acclimate for >12 h prior to the addition of AZA-1 (1 or 10 nM final) or equivalent amounts of methanolic vehicle (0.1% final). Cells were harvested for RNA extractions at 1, 4, and 24 h and for protein and cholesterol extractions at 4, 12, and 24 h.

RNA processing

Immediately following centrifugation at 1000 ×*g* for 5 min, cells were disrupted by resuspending in 1 ml Tri-Reagent (Molecular Research Center, Inc., Cincinnati, OH, USA). All samples were processed according to the manufacturer's protocol. Total RNA was resuspended in DEPC water, purified with a Qiagen RNeasy column (Valencia, CA, USA), and quantified by UV–Vis spectroscopy. The RNA was then qualified on an Agilent 2100 Bioanalyzer (Palo Alto, CA, USA) to confirm the yield of high-quality RNA.

RNA labeling and array hybridization

Four hundred nanograms of total RNA from each time-matched control and treatment sample was amplified separately and labeled with either Cy3- or Cy5-conjugated CTP (Perkin–Elmer, Boston, MA, USA) with a low input linear amplification kit (Agilent Technologies) according to the manufacturer's protocol. After labeling and cleanup, amplified RNA was quantified by UV–Vis spectroscopy. One microgram each of Cy3- and Cy5-labeled targets were combined and hybridized to an Agilent whole human genome oligonucleotide microarray (Cat. No. G4112A) array for 17 h at 60°C. After hybridization, arrays

were washed consecutively in solutions of 6×SSPE with 0.005% *N*-lauroylsarcosine and 0.06×SSPE with 0.005% *N*-lauroylsarcosine for 1 min each at room temperature, followed by a 30-s rinse in Agilent stabilization and drying solution. Three biological replicates, one of which was used in a dye swap, were performed at the 4- and 24-h time points.

Microarray analysis

Microarrays were imaged using an Agilent microarray scanner. Images were extracted with Agilent Feature Extraction software version A7.5.1 and data analyzed with the Rosetta Resolver 7.0 gene expression analysis system (Rosetta Informatics, Seattle, WA, USA). Using a rank consistency filter, features were subjected to a combination linear and lowess normalization algorithm. Based on the Rosetta error model designed for the Agilent platform, a composite array was generated at each time point, in which the data for each feature underwent a weighted averaging based on feature quality in the triplicate arrays making up the composite. A list of "signature" gene features was then generated for each time point from the composite array by *p* value sorting and absolute differential expression ≥1.5-fold (≥0.58 and ≤−0.58 $\log_2$ ratio values). Gene feature clusters in the trend plots were grouped using a *K*-means algorithm with Euclidean distance measurements for genes with a *p* value $<10^{-4}$.

Quantitative real-time PCR

One microgram of total RNA was reverse transcribed using Ambion's RETROscript kit (Austin, TX, USA) with oligo(dT) primers for the two-step qPCR assays. Gene-specific primers (Supplementary Table 5) were used to amplify message by qPCR using an ABI 7500 with ABI SYBR green master mix (Foster City, CA, USA). All 25 μl qPCRs were run in triplicate and contained 1× SYBR green PCR master mix, 400 nM gene-specific primers, and 1 μl of reverse-transcribed sample. Statistical analyses were performed using JMP software (version 5.1.2; SAS Institute, Inc., Cary, NC, USA). For further details, see Morey et al. [21].

Analysis of microarray and qPCR correlation

The correlation of qPCR with microarray data was analyzed using JMP software (version 5.1.2; SAS Institute, Inc.). All calculations of correlation were performed on the $\log_2$ ratio value from the composite array and the corresponding mean $\log_2$ ratio from qPCR analyses. Because the data were normally distributed Pearson's correlation calculation was used. One-way ANOVAs were then used to determine the relationship between the observed correlations. An α value of 0.05 was used for all tests.

Analysis of cellular signaling pathway alterations

The Gene Map Annotator and Pathway Profiler (GenMAPP) and MAPPFinder analysis softwares were used to examine various cellular signaling pathways for AZA-specific alterations in microarray gene expression [59]. MAPPFinder uses Gene Ontology (GO)-based annotations for displaying and analyzing the gene expression data in the GO hierarchy [60]. GO terms identified in MAPPFinder with high *Z* scores were then used to direct efforts toward signaling pathways of interest illustrated in GenMAPP. *Z* scores were calculated by subtracting the expected number of differentially expressed genes from the observed number and then dividing by the standard deviation of the observed number of genes. A positive *Z* score indicated that there were more genes differentially expressed in a GO term/pathway than would be expected by random chance. All gene expression data, regardless of relative fold change or *p* value, were loaded into the GenMAPP program, in which the data were plotted onto specific biological signaling pathways for visualization. Gene expression was visualized using a color coding system, whereby genes were differentially colored according to up or down regulation, fold change (≤−1.5 or ≥1.5), and *p* value ($p \leq 10^{-4}$).

Immunoblot analysis of LDLR

Cells were pelleted and lysed using ice-cold Extraction Buffer (Stressgen Cat. No. 80–1526) containing a protease inhibitor mixture (EDTA-free; Roche Diagnostics Cat. No. 10481700) and 0.1 mM PMSF. Samples were incubated on ice for 30 min and then cleared by centrifugation at 15,000 ×*g* for 10 min at 4°C. Protein concentrations of the extracts were determined by the BCA protein assay (Pierce). Equal amounts of protein (30 to 40 μg) were run under reducing conditions on NuPAGE 3–8% Tris–acetate gels (Invitrogen) and transferred to pure nitrocellulose membranes. Following transfer, membranes were incubated in 0.2% Ponceau-S in 1 M acetic acid to ensure even loading. Membranes were blocked by incubation in Tris-buffered saline containing 5% nonfat dry milk and 0.1% Tween 20 for 1 h at room temperature, washed three times in Tris-buffered saline, and incubated overnight with the primary antibody at 4°C. Membranes were washed three times with Tris-buffered saline and incubated with the corresponding horseradish peroxidase-conjugated anti-IgG for 1 h at room temperature. LDLR was probed using a biotin-linked antibody (Abcam Cat. No. ab50296) with NeutrAvidin (Pierce Cat. No. 31000) biotin-binding, HRP-conjugated protein. Detection of proteins was achieved by the Western Lightning ECL system (Perkin–Elmer LAS, Inc., Cat. No. NEL102). For relative protein quantification, representative blots were scanned using an Epson Perfection 2450 scanner and analyzed using NIH ImageJ version 1.38x. Significant differences between means were assessed by an ANOVA followed by a Tukey multiple *t*-test where $p<0.001$ were considered significant.

Quantitative analysis of cellular cholesterol by gas chromatography

Cells (2×10^6) from triplicate experimental flasks were pelleted and washed twice in 10 ml phosphate-buffered saline. Cellular cholesterol was extracted and assayed as previously described by Ishikawa et al. [61]. Briefly, pellets were extracted with 5 ml of extraction solution (3 ml hexane, 2 ml 2-propanol) including 5 μg stigmasterol (Sigma Cat. No. S2424) as internal standard for 45 to 60 min. Samples were centrifuged at 1500 ×*g* for 10 min and supernatants were collected and divided into two equal volumes for separate extraction of "free cholesterol" and "total cholesterol" and then dried under nitrogen. Free cholesterol samples were immediately resuspended in chloroform (200 μl) and prepared for GC injection. Total cholesterol samples were resuspended in 100 μl tetramethylammonium hydroxide (Sigma Cat. No. 334901; 25% in 2-propanol) and incubated at 80°C for 20 min. Samples were vortexed and 50 μl of tetrachloroethylene/methylbutyrate (1:3; Sigma Cat. Nos. 270393 and 246093) solution and 200 μl Milli-Q water were added. Samples were centrifuged at 2500 ×*g* and the lipid-soluble fractions were collected for GC injection.

Cholesterol quantification was carried out on an Agilent Technologies Model 6890N gas chromatograph system outfitted with a Model DB-17 capillary column (J&W Scientific Cat. No. 125–1712). Total and free cholesterol data were normalized to cell number (hemocytometer and Coulter counter counts) and cellular protein. Significant differences between means were assessed by an ANOVA followed by a Tukey multiple *t*-test where $p<0.001$ were considered significant.

Acknowledgments

Funding for the Marine Institute, Ireland, was obtained from the Irish National Development Plan under Marine Research Strategic Project ST-02-02, Azaspiracids Standards and Toxicology. M.J.T. was supported by a National Research Council Associateship Award through NOAA/NOS/NCCOS/CCEHBR. S.M.H. was supported by NIH Grant HL079274 and the South Carolina COBRE in Lipidomics and Pathobiology (P20 RR17677 from NCRR). The authors thank Arjen Gerssen for his help with ChemDraw and Dr. Richard Klein and Charlyne Chassereau for their technical assistance with cholesterol gas chromatography.

Appendix A. Supplementary data

Supplementary data associated with this article can be found, in the online version, at doi:10.1016/j.ygeno.2007.10.015.

References

[1] P. Hess, T. McMahon, D. Slattery, D. Swords, G. Dowling, M. McCarron, D. Clarke, W. Gibbons, J. Silke, M. O'Cinneide, Use of LC-MS testing to identify lipophilic toxins, to establish local trends and interspecies differences and to test the comparability of LC-MS testing with the mouse bioassay: an example from the Irish Biotoxin Monitoring Programme 2001. Molluscan Shellfish Safety, Proceedings of the Fourth International Conference on Molluscan Shellfish Safety, Consellería de Pesca e Asuntos Marítimos da Xunta de Galicia, and Intergovernmental Oceanographic Commission of UNESCO, Santiago de Compostella, 2003, pp. 57–65.

[2] A. Furey, C. Moroney, A.B. Magdalena, M.J.F. Saez, M. Lehane, K.J. James, Geographical, temporal, and species variation of the polyether toxins, azaspiracids, in shellfish, Environ. Sci. Technol. 37 (2003) 3078–3084.

[3] P. Hess, T. McMahon, D. Slattery, D. Swords, G. Dowling, M. McCarron, D. Clarke, L. Devilly, W. Gibbons, J. Silke, M. O'Cinneide, Biotoxin chemical monitoring in Ireland 2001, Proceedings of the Second Irish Marine Science Biotoxin Workshop, Marine Institute, Dublin, 2001, pp. 8–18.

[4] M. Satake, K. Ofuji, K.J. James, A. Furey, T. Yasumoto, New toxic event caused by Irish mussels, in: B. Reguera, J. Blanco, M.L. Fernandez, T. Wyatt (Eds.), Harmful Algae, Xunta de Galicia and Intergovernmental Oceanographic Commission of UNESCO, Santiago de Compostella, 1998, pp. 468–469.

[5] E. Ito, M. Satake, K. Ofuji, M. Higashi, K. Harigaya, T. McMahon, T. Yasumoto, Chronic effects in mice caused by oral administration of sublethal doses of azaspiracid, a new marine toxin isolated from mussels, Toxicon 40 (2002) 193–203.

[6] K.J. James, A. Furey, M. Lehane, H. Ramstad, T. Aune, P. Hovgaard, S. Morris, W. Higman, M. Satake, T. Yasumoto, First evidence of an extensive northern European distribution of azaspiracid poisoning (AZP) toxins in shellfish, Toxicon 40 (2002) 909–915.

[7] A.B. Magdalena, M. Lehane, S. Krys, M.L. Fernandez, A. Furey, K.J. James, The first identification of azaspiracids in shellfish from France and Spain, Toxicon 42 (2003) 105–108.

[8] H. Taleb, P. Vale, R. Amanhir, A. Benhadouch, R. Sagou, A. Chafik, First detection of azaspiracids in mussels in north west Africa, J. Shellfish Res. 25 (2006) 1067–1070.

[9] P. Hess, P. McCarron, N. Rehmann, J. Kilcoyne, T. McMahon, G. Ryan, P.M. Ryan, M.J. Twiner, G.J. Doucette, E. Ito, T. Yasumoto, Isolation and purification of azaspiracids from naturally contaminated materials, and evaluation of their toxicological effects—final project report ASTOX (ST/02/02), Marine Institute: Marine Environment & Health Series, 2007, p. 129.

[10] T. McMahon, J. Silke, Re-occurrence of winter toxicity, Harm. Algae News 17 (1998) 12.

[11] T. McMahon, J. Silke, Winter toxicity of unknown aetiology in mussels, Harm. Algae News 14 (1996) 2.

[12] K. Ofuji, M. Satake, T. McMahon, J. Silke, K.J. James, H. Naoki, Y. Oshima, T. Yasumoto, Two analogs of azaspiracid isolated from mussels, *Mytilus edulis,* involved in human intoxication in Ireland, Nat. Toxins 7 (1999) 99–102.

[13] E. Ito, K. Terao, T. McMahon, J. Silke, T. Yasumoto, Acute pathological changes in mice caused by crude extracts of novel toxins isolated from Irish mussels, in: B. Reguera, J. Blanco, M.L. Fernandez, T. Wyatt (Eds.), Harmful Algae, Xunta de Galicia and Intergovernmental Oceanographic Commission of UNESCO, Santiago de Compostella, 1998, pp. 588–589.

[14] E. Ito, M. Satake, K. Ofuji, N. Kurita, T. McMahon, K. James, T. Yasumoto, Multiple organ damage caused by a new toxin azaspiracid, isolated from mussels produced in Ireland, Toxicon 38 (2000) 917–930.

[15] J.R. Colman, M.J. Twiner, P. Hess, T. McMahon, M. Satake, T. Yasumoto, G.J. Doucette, J.S. Ramsdell, Teratogenic effects of azaspiracid-1 identified by microinjection of Japanese medaka (*Oryzias latipes*) embryos, Toxicon 45 (2005) 881–890.

[16] M.J. Twiner, P. Hess, M.-Y. Bottein Dechraoui, T. McMahon, M.S. Samons, M. Satake, T. Yasumoto, J.S. Ramsdell, G.J. Doucette, Cytotoxic and cytoskeletal effects of azaspiracid-1 on mammalian cell lines, Toxicon 45 (2005) 891–900.

[17] E. Ito, M.O. Frederick, T.V. Koftis, W. Tang, G. Petrovic, T. Ling, K.C. Nicolaou, Structure toxicity relationships of synthetic azaspiracid-1 and analogs in mice, Harmful Algae News 5 (2006) 586–591.

[18] Y. Roman, A. Alfonso, M.C. Louzao, L.A. de la Rosa, F. Leira, J.M. Vieites, M.R. Vieytes, K. Ofuji, M. Satake, T. Yasumoto, L.M. Botana, Azaspiracid-1, a potent, nonapoptotic new phycotoxin with several cell targets, Cell Signal. 14 (2002) 703–716.

[19] N. Vilarino, K.C. Nicolaou, M.O. Frederick, E. Cagide, I.R. Ares, M.C. Louzao, M.R. Vieytes, L.M. Botana, Cell growth inhibition and actin cytoskeleton disorganization induced by azaspiracid-1 structure–activity studies, Chem. Res. Toxicol. 19 (2006) 1459–1466.

[20] G. Ronzitti, P. Hess, N. Rehmann, G.P. Rossini, Azaspiracid-1 alters the E-cadherin pool in epithelial cells, Toxicol. Sci. 95 (2007) 427–435.

[21] J. Morey, J. Ryan, F. Van Dolah, Microarray validation: factors influencing correlation between inkjet printed oligonucleotide microarrays and real-time PCR, Biol. Proced. Online 8 (2006) 175–193.

[22] S. Morikawa, T. Murakami, H. Yamazaki, A. Izumi, Y. Saito, T. Hamakubo, T. Kodama, Analysis of the global RNA expression profiles of skeletal muscle cells treated with statins, J. Atheroscler. Thromb. 12 (2005) 121–131.

[23] W.H. Frishman, R.C. Rapier, Lovastatin: an HMG-CoA reductase inhibitor for lowering cholesterol, Med. Clin. North Am. 73 (1989) 437–448.

[24] A. Endo, M. Kuroda, Y. Tsujita, ML-236A, ML-236B, and ML-236C, new inhibitors of cholesterogenesis produced by *Penicillium citrinium*, J. Antibiot. (Tokyo) 29 (1976) 1346–1348.

[25] M. Cassader, G. Ruiu, R. Gambino, N. Alemanno, F. Veglia, G. Pagano, Hypercholesterolemia in non-insulin-dependent diabetes mellitus: different effect of simvastatin on VLDL and LDL cholesterol levels, Atherosclerosis 99 (1993) 47–53.

[26] L.M. Olivier, K.L. Chambliss, K.M. Gibson, S.K. Krisans, Characterization of phosphomevalonate kinase: chromosomal localization, regulation, and subcellular targeting, J. Lipid Res. 40 (1999) 672–679.

[27] L.J. Engelking, G. Liang, R.E. Hammer, K. Takaishi, H. Kuriyama, B.M. Evers, W.-P. Li, J.D. Horton, J.L. Goldstein, M.S. Brown, Schoenheimer effect explained—feedback regulation of cholesterol synthesis in mice mediated by Insig proteins, J. Clin. Invest. 115 (2005) 2489–2498.

[28] D. Eberle, B. Hegarty, P. Bossard, P. Ferre, F. Foufelle, SREBP transcription factors: master regulators of lipid homeostasis, Biochimie 86 (2004) 839–848.

[29] B.-L. Song, N.B. Javitt, R.A. DeBose-Boyd, Insig-mediated degradation of HMG CoA reductase stimulated by lanosterol, an intermediate in the synthesis of cholesterol, Cell Metab. 1 (2005) 179–189.

[30] J.D. Horton, J.L. Goldstein, M.S. Brown, SREBPs: activators of the complete program of cholesterol and fatty acid synthesis in the liver, J. Clin. Invest. 109 (2002) 1125–1131.

[31] D. Cunningham, D. Swartzlander, S. Liyanarachchi, R.V. Davuluri, G.E. Herman, Changes in gene expression associated with loss of function of the NSDHL sterol dehydrogenase in mouse embryonic fibroblasts, J. Lipid Res. 46 (2005) 1150–1162.

[32] A. Helip-Wooley, J.G. Thoene, Sucrose-induced vacuolation results in increased expression of cholesterol biosynthesis and lysosomal genes, Exp. Cell Res. 292 (2004) 89–100.

[33] X. Wang, M. Chamberlain, O. Vassieva, C. Henderson, C. Wolf, Relationship between hepatic phenotype and changes in gene expression in cytochrome P450 reductase (POR) null mice, Biochem. J. 388 (2005) 857–867.

[34] L. Weber, M. Boll, A. Stampfl, Maintaining cholesterol homeostasis: sterol regulatory element-binding proteins, World J. Gastroenterol. 10 (2004) 3081–3087.

[35] N. Sekar, J.D. Veldhuis, Involvement of Sp1 and SREBP-1a in transcriptional activation of the LDL receptor gene by insulin and LH in cultured porcine granulosa–luteal cells, Am. J. Physiol., Endocrinol. Metab. 287 (2004) E128–E135.

[36] E.D. Rosen, C.J. Walkey, P. Puigserver, B.M. Spiegelman, Transcriptional regulation of adipogenesis, Genes Dev. 14 (2000) 1293–1307.

[37] D. Lambert, C.A. O'Neill, P.J. Padfield, Depletion of Caco-2 cell cholesterol disrupts barrier function by altering the detergent solubility

and distribution of specific tight-junction proteins, Biochem. J. 387 (2005) 553–560.
[38] S.-H. Koo, L. Flechner, L. Qi, X. Zhang, R.A. Screaton, S. Jeffries, S. Hedrick, W. Xu, F. Boussouar, P. Brindle, H. Takemori, M. Montminy, The CREB coactivator TORC2 is a key regulator of fasting glucose metabolism, Nature 437 (2005) 1109–1111.
[39] N. Abrahamsen, K. Lundgren, E. Nishimura, Regulation of glucagon receptor mRNA in cultured primary rat hepatocytes by glucose and cAMP, J. Biol. Chem. 270 (1995) 15853–15857.
[40] K. Chu, M.-J. Tsai, Neuronatin, a downstream target of BETA2/NeuroD1 in the pancreas, is involved in glucose-mediated insulin secretion, Diabetes 54 (2005) 1064–1073.
[41] L. Riera, A. Manzano, A. Navarro-Sabate, J.C. Perales, R. Bartrons, Insulin induces PFKFB3 gene expression in HT29 human colon adenocarcinoma cells, Biochim. Biophys. Acta 1589 (2002) 89–92.
[42] S. Herzig, S. Hedrick, I. Morantte, S.-H. Koo, F. Galimi, M. Montminy, CREB controls hepatic lipid metabolism through nuclear hormone receptor PPAR-γ, Nature 426 (2003) 190–193.
[43] D.J. Van Den Berg, A.K. Sharma, E. Bruno, R. Hoffman, Role of members of the Wnt gene family in human hematopoiesis, Blood 92 (1998) 3189–3202.
[44] W.J. Nelson, R. Nusse, Convergence of Wnt, β-catenin, and cadherin pathways, Science 303 (2004) 1483–1487.
[45] R. Nusse, WNT targets: repression and activation, Trend Genet. 15 (1999) 1–3.
[46] X. Zeng, K. Tamai, B. Doble, S. Li, H. Huang, R. Habas, H. Okamura, J. Woodgett, X. He, A dual-kinase mechanism for Wnt co-receptor phosphorylation and activation, Nature 438 (2005) 873–877.
[47] R. Eckert, A. Broome, M. Ruse, N. Robinson, D. Ryan, K. Lee, S100 proteins in the epidermis, J. Invest. Dermatol. 123 (2004) 23–33.
[48] S.C. Garrett, K.M. Varney, D.J. Weber, A.R. Bresnick, S100A4, a mediator of metastasis, J. Biol. Chem. 281 (2006) 677–680.
[49] N. Comes, X. Gasull, A. Gual, T. Borras, Differential expression of the human chloride channel genes in the trabecular meshwork under stress conditions, Exp. Eye Res. 80 (2005) 801–813.
[50] Y.-P. Dai, S. Bongalon, W.J. Hatton, J.R. Hume, I.A. Yamboliev, ClC-3 chloride channel is upregulated by hypertrophy and inflammation in rat and canine pulmonary artery, Br. J. Pharmacol. 145 (2005) 5–14.
[51] G. Buyse, D. Trouet, T. Voets, L. Missiaen, G. Droogmans, B. Nilius, J. Eggermont, Evidence for the intracellular location of chloride channel (ClC)-type proteins: co-localization of ClC-6a and ClC-6c with the sarco/endoplasmic-reticulum Ca^{2+}pump SERCA2b, Biochem. J. 330 (1998) 1015–1021.
[52] A. Alfonso, Y. Roman, M.R. Vieytes, K. Ofuji, M. Satake, T. Yasumoto, L.M. Botana, Azaspiracid-4 inhibits Ca^{2+}entry by stored operated channels in human T lymphocytes, Biochem. Pharmacol. 69 (2005) 1627–1636.
[53] Y. Roman, A. Alfonso, M.R. Vieytes, K. Ofuji, M. Satake, T. Yasumoto, L.M. Botana, Effects of azaspiracids 2 and 3 on intracellular cAMP, [Ca^{2+}], and pH, Chem. Res. Toxicol. 17 (2004) 1338–1349.
[54] K.V. Kulagina, M.J. Twiner, P. Hess, T. McMahon, M. Satake, T. Yasumoto, J.S. Ramsdell, G.J. Doucette, W. Ma, T.J. O'Shaughnessy, Azaspiracid-1 inhibits bioelectrical activity of spinal cord neuronal networks, Toxicon 47 (2006) 766–773.
[55] A. Gulacsi, C.R. Lee, A. Sik, T. Viitanen, K. Kaila, J.M. Tepper, T.F. Freund, Cell type-specific differences in chloride-regulatory mechanisms and $GABA_A$ receptor-mediated inhibition in rat substantia nigra, J. Neurosci. 23 (2003) 8237–8246.
[56] M.C. Horne, G.L. Goolsby, K.L. Donaldson, D. Tran, M. Neubauer, A.F. Wahl, Cyclin G1 and cyclin G2 comprise a new family of cyclins with contrasting tissue-specific and cell cycle-regulated expression, J. Biol. Chem. 271 (1996) 6050–6061.
[57] T. Jacks, R.A. Weinberg, Cell-cycle control and its watchman, Nature 381 (1996) 643–644.
[58] M.C. Horne, K.L. Donaldson, G.L. Goolsby, D. Tran, M. Mulheisen, J.W. Hell, A.F. Wahl, Cyclin G2 is up-regulated during growth inhibition and B cell antigen receptor-mediated cell cycle arrest, J. Biol. Chem. 272 (1997) 12650–12661.
[59] K.D. Dahlquist, N. Salomonis, K. Vranizan, S.C. Lawlor, B.R. Conklin, GenMAPP, a new tool for viewing and analyzing microarray data on biological pathways, Nat. Genet. 31 (2002) 19–20.
[60] S. Doniger, N. Salomonis, K. Dahlquist, K. Vranizan, S. Lawlor, B. Conklin, MAPPFinder: using Gene Ontology and GenMAPP to create a global gene-expression profile from microarray data, Genome Biol. 4 (2003) R7.
[61] T.T. Ishikawa, J. MacGee, J.A. Morrison, C.J. Glueck, Quantitative analysis of cholesterol in 5 to 20 μl of plasma, J. Lipid Res. 15 (1974) 286–291.